Fungal Biology 123 (2019) 638–649

Contents lists available at ScienceDirect

Fungal Biology

journal homepage: www.elsevier.com/locate/funbio

The central role of septa in the basidiomycete *Schizophyllum commune* hyphal morphogenesis

Marjatta Raudaskoski

Molecular Plant Biology, Department of Biochemistry, University of Turku, FI-20014 Turku, Finland

ARTICLE INFO

Article history:
Received 18 February 2019
Received in revised form
10 May 2019
Accepted 13 May 2019
Available online 22 May 2019

Corresponding Editor: Steven Bates

Keywords:
Contractile actin ring
Disruption of actin cytoskeleton
Filamentous basidiomycetes
Nuclear division and movements
Septum

ABSTRACT

The purpose of the present research was to observe in the filamentous basidiomycete *Schizophyllum commune*, the connection between the nuclear division and polymerization of the contractile actin ring with subsequent formation of septa in living hyphae. The filamentous actin was visualized using Lifeact-mCherry and the nuclei with EGFP tagged histone 2B (H2B). Time-lapse fluorescence microscopy confirmed that in monokaryotic and dikaryotic hyphae, the first signs of the contractile actin ring occur at the site of the nuclear division, in one to two minutes after division. At this stage, the telophase nuclei have moved tens of micrometers from the division site. The actin ring is replaced by the septum in six minutes. The apical cells treated with filamentous actin disrupting drug latrunculin A, had swollen tips but the cells were longer than in control samples due to the absence of the actin rings. The nuclear pairing and association with clamp cell development as well as the clamp cell fusion with the subapical cell was disrupted in latrunculin-treated dikaryotic hyphae, indicating that actin filaments are involved in these processes, also regulated by the A and B mating-type genes. This suggests that the actin cytoskeleton may indirectly be a target for mating-type genes.

1. Introduction

Recently, fungal cell biology has obtained ample attention due to the availability of the whole genome sequences and the development of live cell imaging of the proteins encoded by central genes that regulate polarized growth, septal morphogenesis and mycelial differentiation (Riquelme et al., 2018; Steinberg et al., 2017). In this advanced research, the filamentous basidiomycetes have received less attention than filamentous ascomycetes, although whole genome sequences of several filamentous basidiomycetes are also available. Recently, however, live cell imaging has been applied to filamentous basidiomycete *Schizophyllum commune* (Jung et al., 2018), which has made it possible to investigate the unique cell biological features of the living hyphae of this fungus and to compare the results with those obtained by traditional cell biological methods.

In filamentous basidiomycetes the hyphae are either haploid, mainly with one nucleus (monokaryotic), or dikaryotic, with two nuclei per hyphal cell. The exception from this rule is the formation of the dikaryon from the mating of haploid hyphae. A process controlled by *A* and *B* mating-type genes (Raper, 1966). The establishment of the dikaryotic phase, with two genetically different nuclei in each cell, requires an extensive reciprocal exchange and the migration of nuclei between the compatible haploid strains with different *A* and *B* genes. This process is regulated by the *B* mating-type genes encoding G protein-coupled receptors and pheromones (Raudaskoski and Kothe, 2010; Raudaskoski, 2015). The nuclear exchange and migration ends with pairing of nuclei with different mating-type genes. In a majority of filamentous basidiomycetes, the synchronous division of the nuclear pair takes place in association with clamp cell formation. This process is regulated by the *A* mating-type genes encoding homeodomain transcription factors. Only the final step in clamp cell formation, the fusion of the clamp cell tip with the subapical cell, requires the presence of different *B* mating-type genes.

In monokaryotic (haploid, homokaryotic) and dikaryotic hyphae of the filamentous basidiomycete *S. commune*, the formation of the septum occurs after nuclear division. The live cell imaging of *S. commune* dikaryotic hyphae with Lifeact-EGFP suggested that the actin cytoskeleton plays a significant role in the location of the nuclear pair at the site of the developing clamp cell, in the growth of the clamp cell and, after nuclear division, in the contractile actin ring formation preceding the septum formation (Jung et al., 2018).

E-mail address: marrau@utu.fi.

https://doi.org/10.1016/j.funbio.2019.05.009
1878-6146/

These results were based on observing H2B::EGFP-labeled nuclei and Lifeact-EGFP-labeled filamentous actin in different hyphae but at the same developmental stage (Jung et al., 2018). In the present work, the nuclear division and actin are visualized in the same hypha with 2HB::EGFP and Lifeact-mCherry, respectively, allowing the detailed recording of the relationship between nuclear division and septal formation in monokaryotic and dikaryotic hyphae. In order to confirm the role of filamentous actin in different processes, Latrunculin A-mediated filamentous actin disruption was applied. Interestingly, during recovery of the hyphae from the Latrunculin A treatment, the nuclear divisions took place without immediate septal formation, which led to changes in the nuclear number of the hyphal cells and to an unbalanced relationship between the nuclei with different mating-type genes in the treated dikaryotic hyphae, which was also reflected in the hyphal morphology.

2. Material and methods

2.1. Strains and culture medium

Monokaryotic (haploid) and dikaryotic strains used in the present study are listed in Table 1. The strains were grown on complete medium (Raper and Raudaskoski, 1968) supplemented with 1% glucose at 29 °C in darkness. For fruiting body production the matings were brought into light at room temperature after 4 days' growth in dark (Raudaskoski and Yli-Mattila, 1985). Mycelia used for microscopic analyses were grown for 24–36 h on cellophane membranes covered with 0.5% agarose in distilled water and overlaying the solid complete medium.

2.2. Cloning and transformation

The hyphal strains expressing H2B::EGFP originated from the previous study (Jung et al., 2018). The strains expressing Lifeact-mCherry were constructed in the present investigation. The primers for mCherry (Clontech, CatNo 632542) cloning were mCherryF GGGGATCCACCGGTCGCCACCAATGGTGAGCAAGGG and mCherryR GCGCGGCCGCGAGACTAGTTTCCGGACTTG with BamHI and Not I restriction sites. The amplified PCR product, containing a linker of seven amino acids (G, N, P, P, V, A, T) in front of mCherry was cloned into the pCR2.1 TOPO vector (Invitrogen). The fragment, consisting of 889 bp of *S. commune* β-tubulin promoter linked to the sequence encoding 17 amino acids of Lifeact was cut with BamH I from p 1–15 (Jung et al., 2018) and cloned into the BamHI opened TOPO vector in front of the linker-mCherry sequence. The short terminator sequence from p 1–15- was cut with Not I and cloned into the Not I restriction site in the vector with the β-tubulin promoter-Lifeact-Linker-mCherry construct. Finally the phleomycin cassette (Schuren and Wessels, 1994) was cloned at the Apa I site in the vector, which was named pLifeact-mCherry. The linearized plasmid was transformed into protoplasts prepared from monokaryotic (haploid) ura-9 and ura-7 strains (Weber et al., 2005; Jung et al., 2018) and the selection was made on complete medium containing 20 μg ml^{-1} phleomycin. The transformants were screened for mCherry fluorescence and several transformants were obtained from each transformation, out of which ura-9-1Lifeact-mCherry and ura-7-3 Lifeact-mCherry (Table 1) were used in the present work.

2.3. Latrunculin A treatments

Latrunculin A (Cayman Chemical Company) dissolved in ethanol (250 μg in 250 μl) was diluted in melted complete medium to an 8 μM concentration. From previous experiments it was known that the same amount of swollen hyphal tips is obtained after 1 h treatment using 8, 16 and 32 μM concentrations of Latrunculin A (Lat A) in solidified complete medium. For Lat A treatments a small inoculum from the edge of an actively growing mycelial colony was cut out with a 100 μl pipette tip and transferred to a cellophane membrane covered with a thin layer of 0.5% agarose in distilled water and overlaying complete medium. The 24–30 h old small colonies grown on the membranes were positioned hyphae downwards on complete medium containing 8 μM Lat A and kept in contact with the drug medium for 1 and 2 h. As controls, similar colonies were moved to complete medium without the drug to reveal the effects of transfer process on the hyphal growth. The transfer or ethanol used for dissolving Lat A had no effect on the hyphal tip growth. After the drug treatment, the membrane with

Table 1
Schizophyllum commune strains used in the present study.

Strains	Genotypes	Applied	Reference
Monokaryons (Haploids)	Mating-type and other relevant genes	In the present research	
684	*A26 B26*	Dikaryon synthesis	Raudaskoski and Yli-Mattila (1985)
1792-114-10	*A43 Bα3-β6*	Lat A treatment and recovery, dikaryon synthesis, IIF microscopy of microtubules	Weber et al. (2005)
ura-9	*A26 Bα4-β1 ura⁻*	Transformation	Jung et al. (2018)
ura-7	*A43 Bα3-β6 ura⁻*	Transformation	This study
I-11H2B::EGFP	*A26 Bα4-β1 ura- h2B::egfp phleom⁺*	Development of septa in dikaryon confocal images	Jung et al. (2018)
4H2B::EGFP	*A43 Bα3-β6 ura⁻ h2B::egfp phloem⁺*	Visualization of nuclei in dikaryon	This study
ura-9-1 Lifeact-mCerry	*A26 Bα4-β1 ura-1 ptub3 lifeact-linker mCherry-st phleom+*	Visualization of septa in dikaryon	This study
ura-7-3Lifeact-mCherry	*A43 Bα3-β6 ura⁻ ptub3lifeact-linker mCherry-st phleom+*	Visualization of septa in haploid and dikaryotic strains	
H2 H2B::EGFP Lifeact-mCherry	*A43 Bα4-β1 h2B::egfp ptub3 lifeact-linker mCherry-st phleom⁺*	Visualization of nuclei and septa in a haploid strain	This study
Dikaryons			
4H2B::EGFP × ura-9-1 Lifeact-mCherry	see above	Visualization of nuclei and septal development in dikaryon epifluorescence	This study
1–11H2B::EGFP × ura-7-3 Lifeact-mCherry	See above	Visualization of nuclei and septal development in dikaryon confocal microcopy, LA-treatment and recovery	This study
H 1792-114-10 × 684	See above	LA treatment and recovery, IIF microscopy of microtubules	This study

the hyphal colony was either examined immediately, fixed or moved hyphae upwards to new complete medium without the drug. After 3–5 min transfers to remove the drug, the hyphal colony was left to recover for 2, 4 and 8 h on complete medium.

2.4. Microscopy

For live cell imaging the thin layer of agarose with the hyphae was carefully separated from the cellophane membrane in distilled water on a microscope slide, placed over with a cover glass and used immediately for microscopy. The Lat A-treated and recovery samples as well as the controls were also fixed with 3.6% formaldehyde in PBS pH 7.0 for 2 h. After rinsing several times in PBS pH 7.0, the hyphae were stained with DAPI (4′, 6-diamidino-2-phenylindole, Sigma, 1 μg ml^{-1}) Hoechst 33342 (Thermo Scientific, 1 μg ml^{-1}) or calcofluor white (Polysciences, 1 μg ml^{-1}). The preparation for indirect immunofluorescence microscopy was performed as reported in Weber et al. (2005).

Bright field and epifluorescence microscopy was performed using a Leitz Orthoplan Large Field Research Microscope (Ernst Leitz GmbH, WetzlaR, Germany) equipped with a 4-lambda Reflected Light Fluorescence Illuminator, a 100 W mercury lamp, and with the proper filter sets for DAPI, Hoechst, calcofluor white, EGFP and mCherry. The cells were examined with the 100× oil immersion objective and images were acquired with a Leica DFC420C color CCD camera (Leica Microsystems Ltd., Heerbrugg, Switzerland). The brightness and contrast of all the digital images was optimized using Corel PhotoPaint and CorelDRAW X7.

Images of living hyphae were also obtained under a confocal microscope, Leica TCS SP5 (Leica Microsystems CMS GmbH, Mannheim, Germany), equipped with the inverted microscope Leica DMI 6000B and an immersion water objective Leica HCX PL APO 63×/1.20 W CORR CS. The lasers used were Ar-laser, excitation line 488 nm for EGFP, and Diode Pumped Solid State (DPSS)-laser, excitation line 561 nm for mCherry.

2.5. Recording of hyphal length and nuclear number

Monokaryotic and dikaryotic hyphae grown for 1 or 2 h on control or 8 μm Lat A containing complete medium were fixed. To measure the apical cell length of leading hyphae, about ten regions

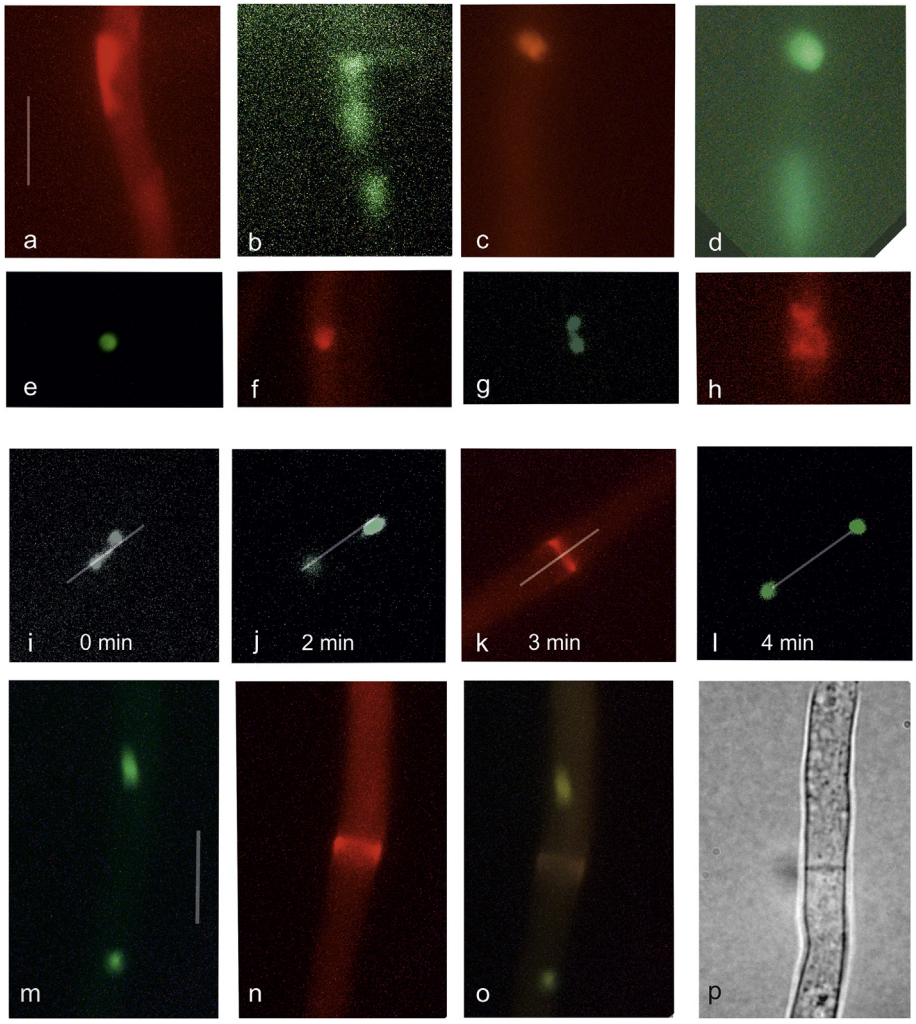

Fig. 1. Nuclear division and septation in living monokaryotic (haploid) hyphae of *Schizophyllum commune*. (a–d) Lifeact-mCherry (a, c) next to H2B::EGFP expressing nuclei (b, d) at onset of division. (e–h) Lifeact-mCherry visualizes actin cytoskeleton (f, h) next to a nucleus with fully condensed chromatin (e) and at late anaphase/early telophase (g). (i–k) Late anaphase (i) and telophase (j) nuclear pair and the contracting actin ring (k) between telophase nuclei about ten μm apart, images recorded at 1 min intervals. The 10 μm line shows that the distance between the telophase nuclei from (j) to (l). The distance between telophase nuclei in (l) increased only a few μm during 4 min recording, probably due to experimental conditions. (m–p) A hypha with telophase nuclei about 20 μm apart (m) and the contractile acting ring in the middle (n). (○) Overlay of m and n. One minute later the apical nucleus (at the top) was 57 μm and the subapical nucleus 33 μm from the contracting actin ring (Suppl. data Fig. 1). (p) Bright field microscopy of the cross wall at the site of the ring 6 min later. Bar 10 μm.

from each colony edge were photographed under a 10× objective in bright field and the apical cell length of the leading hyphae were measured in CorelDraw. In control and Lat A-treated dikaryotic hyphae, the clamp connection at the end of the apical cell was a clear mark for the measurements, while in the control and Lat A-treated apical cells of monokaryotic leading hyphae the septum between the apical and subapical was measured after calcofluor white staining by fluorescence microscopy.

The nuclear number in the apical cells of leading hyphae was counted from 1 to 2 h control and Lat A-treated monokaryotic and dikaryotic hyphae and after 4 h recovery. The nuclei were recorded from fixed and DAPI stained hyphae with 100× oil objective.

3. Results

3.1. Septa are located in the middle of the apical cell

In monokaryotic (haploid) strain 1792-114-10, grown on complete medium at 29 °C, among 40 randomly measured apical cells of leading hyphae, the mean length of longest apical cells (≥300 μm) was 333 ± 25 μm (n = 13), while the length of the shortest ones (≤200 μm) was approximately half of this length 158 ± 32 μm (n = 10). Similarly, in the dikaryon 172-114-10 × 684, the mean length of the longest apical cells (≥200 μm) was 234 ± 30 μm (n = 10) and of the shortest (≤120 μm) close to half of

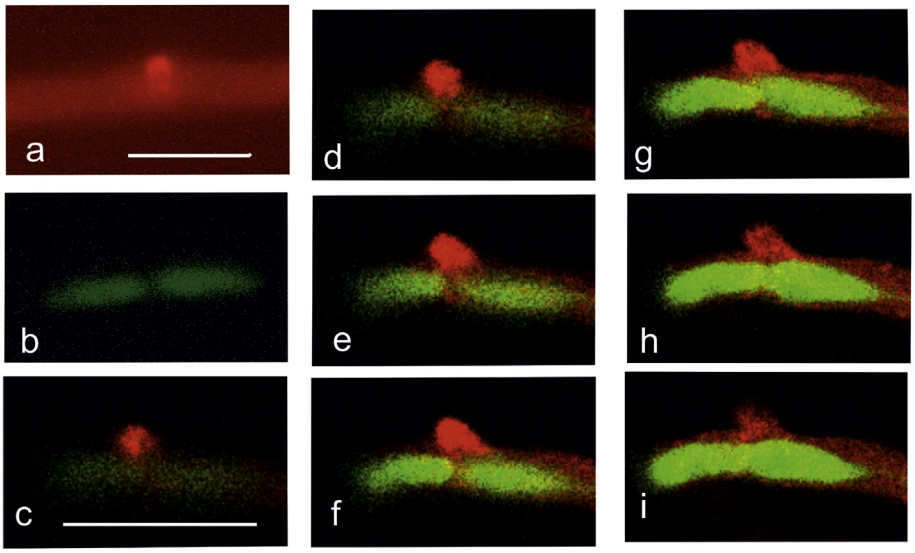

Fig. 2. *Schizophyllum commune* living dikaryotic hyphae. The actin cytoskeleton and nuclei are visualized with Lifeact-mCherry and nuclei with H2B::EGFP, respectively at clamp cell initials. (a–b) With epifluorescence microscopy, actin is seen as a compact spot (a) with the fluorescence of the nuclear pair below (b) at the start of the clamp cell development. (c–i) Seven images (optical planes) with 1 μm intervals from a confocal microscopy z-stack of a clamp cell initial with the nuclear pair. Each image shows different location of Lifeact-mCherry fluorescence in the clamp cell initial and small actin filament fragments in the hypha in association with the nuclei. Bars 10 μm.

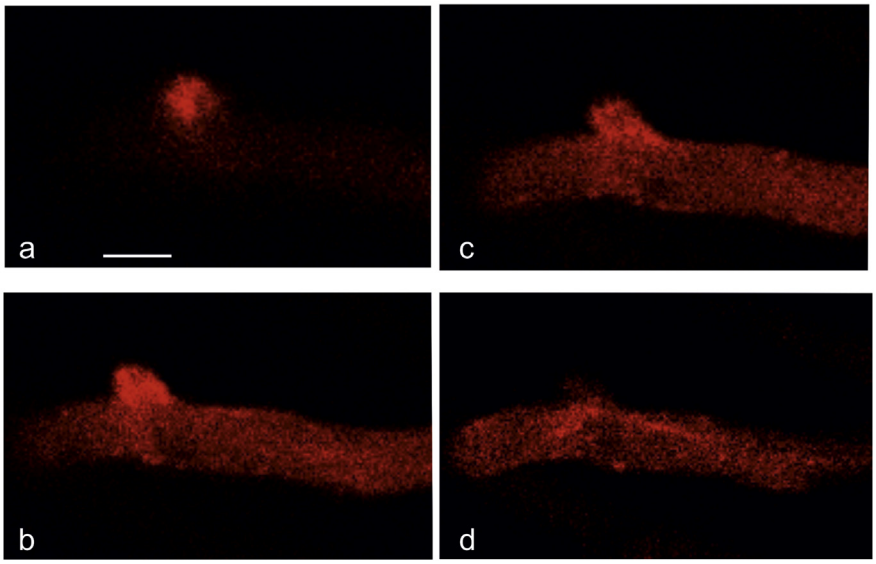

Fig. 3. Actin filaments at high magnification visualized only with Lifeact-mCherry from Fig. 2c, g, and h. (a) Small actin filaments radiate from the center towards the cortex in the clamp cell initial. (b) The actin fluorescence is concentrated at both sides of the clamp initial and some small fragments occur at the site between the nuclei in the hypha (see Fig. 2g). (c) The fluorescent fragments at the neck of the clamp cell initial extend into the hypha toward the nuclear envelope (see Fig. 2h). (d) Filaments in the hypha on the surface of the nuclei (image not in Fig. 2.) Bar 5 μm.

this length 104 ± 10 (n = 10). The short monokaryotic and dikaryotic cells are those that have just undergone the nuclear division and septal formation process. The numbers indicate that the nuclear division and septal formation takes place in or close to the middle part of the long apical cell, leading to a new short apical cell that continues to extend. It is noteworthy that the extension growth of the apical cell of the leading hyphae varies greatly depending on the genetic background of the strain and environmental conditions during growth (Raudaskoski and Viitanen, 1982), but the nuclear division followed by the septal formation occurs approximately in the middle of the apical cell independent of its extension type.

3.2. Septum formation in monokaryotic hyphae

Basidiospores were collected from fruiting bodies originating from the mating of two compatible monokaryotic (haploid) strains, with one expressing Lifeact-mCherry and the other expressing H2B::EGFP construct (Table 1). Germinated basidiospores showing both nuclear and actin fluorescence were isolated and grown to monokaryotic strains H1 and H2, out of which H2 strain (Table 1) was used in order to investigate the relationship between nuclear division and the formation of septum in the same hypha.

Occasionally, an elongated nucleus (Fig. 1b and d) with Lifeact-mCherry accumulation next to it (Fig. 1a and c) occurred in the central part of a few long apical cells. The elongated nucleus was interpreted to be at the early phase of division. In this phase the condensed chromatin gathers at one end of the nucleus and the rest of the nucleus is left behind (Jung et al., 2018). As a consequence of chromatin condensation, the metaphase nucleus was seen as a compact small structure next to the Lifeact-mCherry accumulation (Fig. 1e and f) which quickly turned into an anaphase nucleus (Fig. 1g) surrounded by actin fluorescence (Fig. 1h). At telophase, when the distance between the separating sister nuclei was about 10 μm (Fig. 1i and j), or 3 min since the first recording of the telophase (Fig. 1i), a clear contractile actin ring was formed between the separating sister nuclei (Fig. 1k and l). The contractile actin ring could be distinguished between telophase nuclei more than 10 μm apart (Fig. 1m–o, Suppl. data Fig. S1), depending on how quickly the telophase nuclei separated. The septum was distinguished at the previous site of the contracting actin ring 6 min later (Fig. 1p).

3.3. Septa formation in dikaryotic hyphae

Two dikaryotic strains were used for the purpose of observing septal formation in living hyphae. Strain 1–11 H2B::EGFP × ura-7-3 Lifeact-mCherry (Table 1) was used in confocal microscopic studies (Figs. 2c–i, 3, 5), and strain 4 H2B::EGFP × ura-9-1Lifeact-mCherry (Table 1) was used for epifluorescence microscopy (Figs. 2a and b, 4, Suppl. data. Fig. S2).

In dikaryotic hyphae, the nuclear division starts when the forward movement of the nuclear pair stops at the site of the developing clamp cell. This phenomenon was suggested to be associated with the actin cytoskeleton in the developing clamp cell and in the hypha below it (Jung et al., 2018). Examining living dikaryotic hyphae at the early stage of nuclear division expressing both H2B::EGFP and Lifeact-mCherry visualized strong actin fluorescence in the developing clamp cell and in the hypha where the

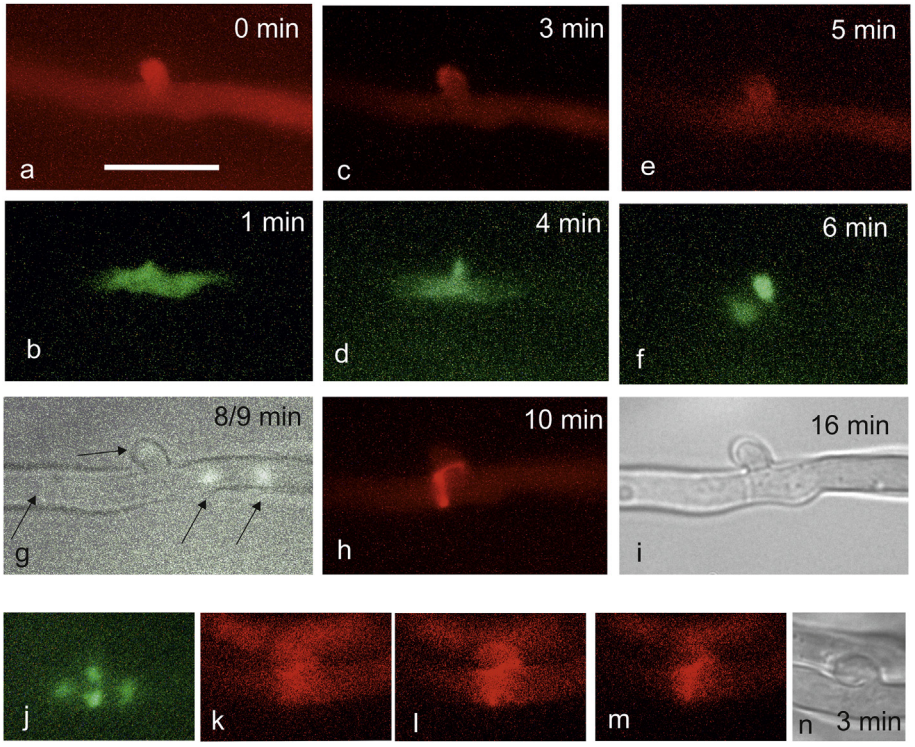

Fig. 4. Nuclear division and septal development in *Schizophyllum commune* living dikaryotic hyphae. (a–i) Time-lapse images recorded for 16 min and (k–m) for about 1 min. The changes in the actin cytoskeleton and the nuclear structure are visualized with Lifeact-mCherry and H2B::EGFP fluorescence, respectively. (a–d) The front nucleus of the pair moves into the clamp cell initial during the first 4 min of division. (e–f) During the next 2 min the nuclei become compact chromatin structures in the clamp cell initial and hypha. (g) In the overlay image of H2B::EGFP (8 min) and bright field (9 min), two telophase nuclei move towards the hyphal apex, one is in the clamp while the fourth nucleus moving toward the subapical cell is not in the plane (arrows). (h) One minute later, Lifeact-mCherry fluorescence shows the contractile actin rings in the hypha and at the base of the clamp cell. (i) Septa replaced the actin rings 6 min later. (j–n) At very early telophase with the four sister nuclei close together (j) strong Lifeact-mCherry fluorescence surrounds the nuclei (k–m) in the hypha and at the base of the clamp cell (n). Bar 10 μm.

nuclear pair was located (Fig. 2a and b). The visualization of the nuclear pair with H2B::EGFP and the actin cytoskeleton with Lifeact-mCherry at a developing clamp cell in successive confocal z-sections with 1 μm intervals (Fig. 2c–i) showed that the Lifeact-mCherry signal varied between different sections of the clamp cell initial and suggested that small fragments with Lifeact-mCherry fluorescence spread from the developing clamp cell towards the nuclei (Fig. 2c–i). When the same *z*-sections were viewed with only Lifeact-mCherry fluorescence at a higher magnification (Fig. 3a–d) it became clearer that the Lifeact-mCherry fluorescence represents short actin filaments spreading into the hypha and towards the nuclear surface.

In the next phase of the nuclear division, one nucleus of the pair moves into the developing clamp cell. In time-lapse fluorescence microscopy, the movement of the nucleus into the developing clamp cell with strong actin fluorescence happened in 6 min (Fig. 4a–f). At the same time, the size of the nucleus decreased due to chromatin condensation and the release of some parts of the nuclear envelope. During the next 2 min, the nuclei divided, and the telophase movement separated the sister nuclei (Fig. 4g). One to 2 min later, the contractile actin ring occurred in the hypha and at the bases of the clamp cell (Fig. 4h). In fact, the contractile actin rings could occur even faster than in one to 2 min, since recording the fluorescence stage of the nuclei and changing the filter block took at least 1 min in the microscopic system used (Suppl. data Fig. S2). The contractile actin rings were replaced by septa 6 min later (Fig. 4i). In a few cases the very early stage of telophase was caught (Fig. 4j) and Lifeact-mCherry positive material was observed between the still closely located sister nuclei (Fig. 4k–m) probably representing growing and bundling actin filaments of the contractile actin ring (Fig. 4k–n).

The changes in the contractile actin ring structures at a clamp cell with an enclosed nucleus were monitored using confocal microscopy until the opening between the clamp cell tip and the subapical cell was formed (Fig. 5). The fluorescence of the contractile actin ring at the base of the clamp cell faded during the first 5 min. The fluorescence of the contractile actin ring in the hypha stayed longer and its fluorescence moved towards the clamp cell tip and the subapical cell fusion site during next 5 min. After 13 min the fluorescence of actin had disappeared and the nucleus from the clamp cell was observed moving into the subapical cell (Fig. 5b and c). During the 12-min recording period the nuclear pair in the apical cell moved about 10 μm towards the hyphal tip (Fig. 5b and c).

3.4. Hyphal structure and nuclear number in hyphae without septa

The mean apical cell lengths at 1 h and 2 h in the monokaryotic and in the dikaryotic control samples were nearly identical (Fig. 6). Instead, the mean apical cell lengths of both the monokaryotic and dikaryotic leading hyphae treated with Lat A for 1 or 2 h were significantly longer compared to the control samples (Fig. 6).The long apical cells in the Lat A-treated samples resulted from the inhibition of the formation of the contractile actin ring necessary for septal formation. The depolymerization of microfilaments by Lat A led to swollen hyphal tips both in the thin and long monokaryotic and thick and short dikaryotic apical cells of the leading hyphae (Fig. 7a,c) and no fluorescence of the actin cytoskeleton was observed in fixed or living swollen hyphal tips (not shown). Staining of control and Lat A-treated hyphae with calcofluor white showed an accumulation of positive material at the swollen hyphal tips and along the apical cell. Such accumulations were not observed in control hyphae (Fig. 7b, d). The transport of calcofluor positive material to the swollen tips could take place along microtubules which were present in the Lat A treated hyphae but in a disorganized manner (Suppl.data Fig. S3). The clamp cell formation

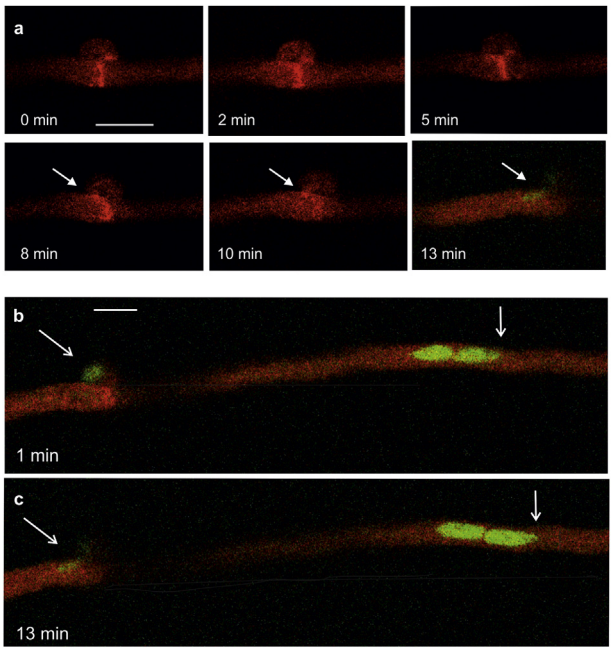

Fig. 5. The dynamics of contractile actin rings and fusion between clamp tip and subapical cell in a living dikaryotic hypha of *Schizophyllum commune*. The examples were chosen from time-lapse scans with Lifeact-mCherry and H2B:EGFP. The time of the contractile ring development and fusion are given from the start to the end of the experiment. The apical cell tip extends towards right of the frame. (a) Both actin rings were visualized for 2 min at the onset of the experiments. After minutes the actin ring at the base of the clamp cell faded but the fluorescence around the ring in hypha remained strong, and some of its fluorescence seemed to move from the ring to the site of the clamp cell fusion with the subapical cell (8 min, arrow).Two minutes later (at 10 min) the fluorescence of the actin ring in the hypha had faded and a bright spot was seen at the fusion site (arrow). Three minutes later (at 13 min) the nucleus moved from the clamp cell into the subapical cell through the opening formed by the fusion (arrow). (b) The nucleus in the clamp cell (oblique arrow) and the nuclear pair in the middle of the apical cell in the second scan (1 min). (c) In the last scan (13 min, the same as the last part in a, but larger) the nucleus is moving from the clamp cell into the subapical cell (oblique arrow) and the nuclear pair in apical cell has proceeded nine μm towards the apical cell tip in 12 min (indicated by the vertical arrows at the tip of the front nucleus in b and c). Bars 10 μm.

was not completely absent from the dikaryotic apical cells, but in 24% of the 1 h and 36% in the 2 h samples treated with Lat A an early stage of clamp cell development without any nucleus, septa or actin fluorescence was recorded in the middle of the apical cell (Fig. 7i).

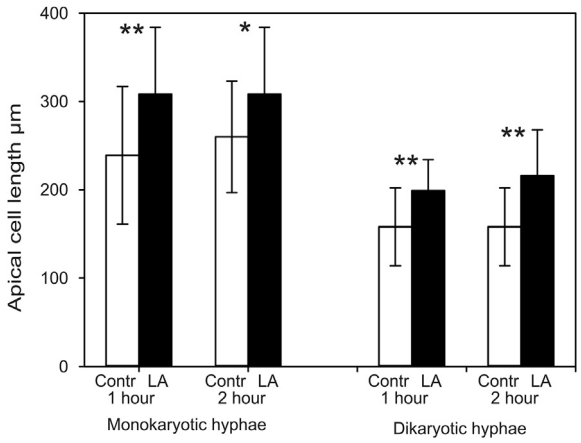

Fig. 6. Mean apical cell length and standard deviation in *Schizophyllum commune* monokaryon 1792-114-10 and dikaryon 1792-114-10 × 684 in control and Lat A-treated samples. The apical cells are significantly longer in 1 and 2 h Lat A-treated than in the control hyphae both in monokaryotic and dikaryotic samples. In each sample 25 apical cells were measured. Student's *t* test $^{*}P \leq 0.05$, $^{**}P \leq 0.01$.

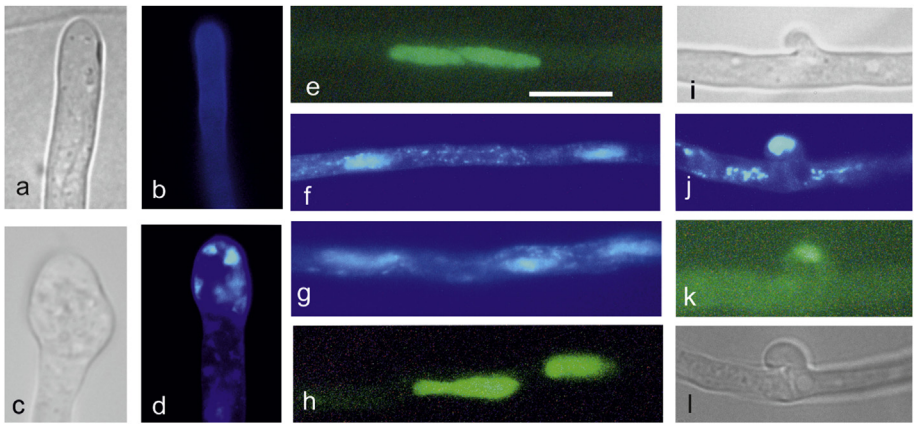

Fig. 7. The morphology and nuclear distribution of *Schizophyllum commune* control (a,b,e) and Lat A-treated hyphae of dikaryons 1792-114-10 × 684 (c,d,f,g,i,j) and 1–11H2:B::EGFP × ura 7-3-Lifeact-mCherry (e,h,k,l). Bright field microscopy (a,c,i,l), fixed and calcofluor white (b,d) and DAPI (f,g,j) stained hyphae and the H2B::EGFP expression of living hyphae (e,h,k). (a) A tip of a control and (c) of an 1 h Lat A-treated hypha. (b) Weak calcofluor white staining of a control hyphal tip and (d) calcofluor white patches in a swollen tip. (e) H2B::EGFP expression of a tightly associated nuclear pair in a control hypha. (f, h) Increased distance between the nuclear pair, (g) three nuclei and (i) a small clamp initial (j,k) in Lat A-treated apical cells. (j,k,l) Unfused clamp connections with trapped nuclei (j.k). In Lat A-treated apical cells. Bar 10 μm.

The nuclear number per apical cell was recorded in both control and Lat A-treated hyphae. In control hyphae, 80–90% of monokaryotic and dikaryotic apical cells had one or two nuclei, respectively. The rest of the apical cells had either two nuclei in haploid or four nuclei in dikaryotic samples representing the division stage of the nuclei (Fig. 8). In Lat A-treated samples, an increase of two or more nuclei in monokaryotic apical cells was recorded, and in the 2 h Lat A-treated dikaryotic samples the number of apical cells with two nuclei decreased while the cells with one, three and four nuclei increased (Figs. 7g and 8).The nuclear number was more stable in the 1 h and 2 h Lat A-treated dikaryotic apical cells than in the treated monokaryotic apical cells (Fig. 8). The close association of the two nuclei with different mating type genes in dikaryotic apical cells (Fig. 7e) was disrupted by Lat A treatment and the nuclei occurred at a distance from each other (Fig. 7f–h). In Lat-A-treated dikaryotic hyphae, the last clamp cells that had formed before treatment often had an enclosed nucleus (Fig. 7j and k). In the case of these clamp cells, a septum occurred both in the hypha and at the base of the clamp connection (Fig. 7l), but the Lat A treatment inhibited the nuclear movement into the subapical cell.

3.5. Recovery from latrunculin A-treatment

During the 4 h recovery from the Lat A treatment the irregular nuclear numbers in the apical cells of monokaryotic and dikaryotic samples increased (Fig. 8). During the early recovery phase (2 h), one or more small tips with polarized growth extended from the swollen apical region, both in the haploid and dikaryotic hyphae (Fig. 9a and b). The calcofluor white positive patches disappeared from the swollen tips, instead, the tips contained one, two or more nuclei not present at the swollen tips during Lat A treatment (Fig. 9c–f, Fig. 10a and b). This indicates that the nuclear transport to the tip was activated once the drug treatment ended. An actin signal in the tip regions was observed in recovering living dikaryotic hyphae by using Lifeact-mCherry (Fig. 10c and d) and indirect immunofluorescence with the actin antibody in fixed haploid hyphae (Fig. 10f). After 4 h of recovery, the nuclei migrated into the polarized branch(es) (Fig. 10e) and after 8 h of recovery, long branches with multiple nuclei extended from the swollen tips (Fig. 9g and h). The increase in nuclear number, indicated that divisions took place during recovery, both in the swollen tips and in the elongating branches. This was supported by the spindle microtubules observed in the fixed haploid and dikaryotic hyphae (Suppl.data Fig. S3). In the multinucleate branches of the swollen tips of dikaryotic hyphae there were observed incomplete clamp cells with associated nuclei and strong actin fluorescence, but without any pairing of nuclei or fluorescence of the contractile actin rings (Figs. 9g and 10h–j). Instead, contractile actin rings occurred in haploid hyphae after 4 h of recovery (Fig. 10g).The full recovery of dikaryotic hyphae was observed after 24 h.

4. Discussion

In the monokaryotic (haploid) and dikaryotic hyphae of *S. commune*, nuclear division associated with septum formation takes place in the middle of a leading apical cell. After nuclear division, the telophase nuclei separate fast and in the new apical cell, the nuclei settle in the middle of the cell where they keep their position in respect to the hyphal apical growth by moving forward with a speed that is relative to the extension speed of the apical cell. These phenomena have been known for a long time, from observing living hyphae under the phase contrast or DIC microscope, in *S. commune* (Snider, 1968), *Polystictus (Trametes) versicolor* (Girbardt, 1968) and *Coprinopsis cinerea* (Kamada and Tanabe, 1995; Tanabe and Kamada, 1996). The nuclear movements were also recently visualized in living hyphae by the help of H2B::EGFP expressing nuclei in *S. commune* (Jung et al., 2018) and the phenomenon was also recorded in the present work. The apical and subapical cells in *S. commune* have an extensive microtubule cytoskeleton with motor proteins, which are responsible for the fast nuclear movements along the microtubules (Raudaskoski, 1998; Raudaskoski et al., 1994, 2009; Brunsch et al., 2015). Instead the role of actin cytoskeleton in hyphal extension, nuclear movements and septum formation has received less attention in filamentous basidiomycetes, although the contractile actin ring was already described in eighties by using NBD phallacidin staining in *S. commune* (Runeberg et al., 1986) and shown to consist of microfilaments by electron microscopic studies in *P. versicolor* (Girbardt, 1979).

4.1. Nuclear division and formation of septa

In the present study the accumulation of Lifeact-mCherry positive material was observed in monokaryotic hyphae next to the nucleus before division. In dikaryotic hyphae, clear actin filaments were recorded in connection with the nuclear surface during the

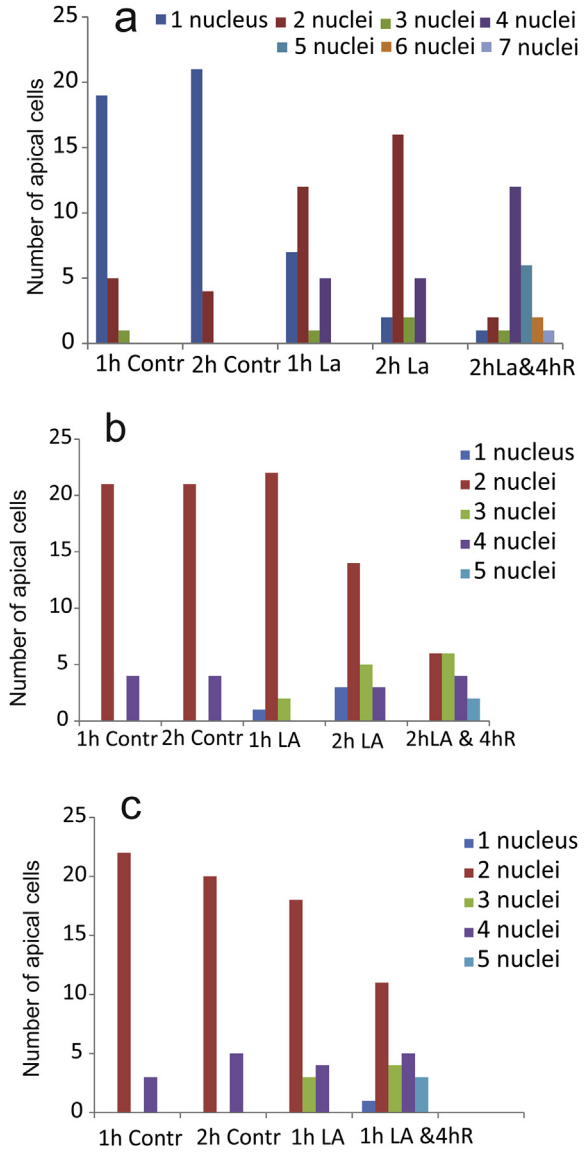

Fig. 8. The nuclear number in control and Lat A -treated *Schizophyllum commune* apical cells. (a) Monokaryotic (haploid) strain 1792-114-10 and dikaryotic strains (b) 1792-114 × 684 and (c) 1–11H2:B::EGFP × ura 7-3-Lifeact-mCherry. In 1 h and 2 h control samples monokaryotic and dikaryotic apical cells regularly contain one or two and two or four nuclei, respectively. In 1 h and 2 h Lat A-treated samples, monokaryotic and dikaryotic apical cells also have 1, 3 and 4 nuclei. After 4 h recovery from Lat A treatment the number of apical cells with irregular nuclear numbers increases both in the monokaryotic and dikaryotic strains. The nuclear number of 25 apical cells was recoded from each sample.

early prophase, when the nuclear pair was located below the developing clamp cell. Fragmented actin filaments also occurred at the sides and in the tip of the developing clamp cells during the movement of one member of the nuclear pair into the growing clamp cell. When the actin cytoskeleton was depolymerized with Lat A, the regular distribution of nuclei in the apical cells was disturbed and no nuclear association with the clamp cell initials nor the formation of a contractile actin ring was observed. These observations support the previous assumption that in dikaryotic hyphae, at the start of mitosis, the nuclei stop their forward movement due to the actin network in the developing clamp cell and beneath it (Jung et al., 2018). The absence of nuclei in the few clamp cell initials in the Lat A-treated dikaryotic hyphae also suggests that in the control hyphae, both the actin cytoskeleton and the microtubule cytoskeleton (Raudaskoski, 1998) are required to regulate the movement of the nucleus into the clamp cell initial for the division process. The actin cytoskeleton could also be involved in the positioning of the nucleus at the site of division in monokaryotic apical cells.

In the multinucleate hyphal compartments of *Aspergillus nidulans*, the formation of septa is also dependent of nuclear division. All nuclei undergo mitosis synchronously, but not all nuclear divisions are followed by septal formation (Taheri-Talesh et al., 2012; Shen et al., 2014). In *Neurospora crassa*, septum formation was observed when the apical cell reached the maximum length of 250 μm and the septum divided the cell into a long apical and shorter subapical part, but the link to nuclear division was not recorded (Delgado-Alvarez et al., 2010, 2014). The septal formation was associated with a tangle of filaments consisting of actin, myosin 2 and tropomyosin. The structure appears at a certain distance from the hyphal tip and migrates forward before forming the contractile actomyosin ring (Delgado-Alvarez et al., 2010, 2014). In *A. nidulans*, strings of myosin (MyoB/myosin 2) appear between nuclei in the area in which septa will form (Taheri-Talesh et al., 2012). In monokaryotic and dikaryotic *S. commune* hyphae, tangled actin filaments were observed between the nuclei at very early telophase, when the nuclei were still very close to each other, and before the first signs of the contractile actin ring had appeared. In dikaryotic hyphae of *S. commune* (Runeberg et al., 1986) and *C. cinerea* (Kamada and Tanabe, 1995; Tanabe and Kamada, 1996), actin has also been shown to concentrate around the dividing nuclei by indirect immunofluorescence microscopy, although the exact division phase was not possible to deduce as it was in the present study with the simultaneous Lifeact-mCherry and H2B::EGFP expression in living hyphae. These observations mean that the actin cytoskeleton remains at the site of nuclear division from early prophase to telophase, and is thus stored at the site for the quick polymerization of the contractile actin ring. In the monokaryotic and dikaryotic hyphae of *S. commune* the association of the nuclear division with the polymerization of the contractile actin ring and the subsequent septa formation appears to be under more stringent control than in ascomycetes.

4.2. Fusion of the clamp cell with the subapical cell

Lifeact-mCherry fluorescence of the contractile actin ring in dikaryotic hyphae appeared in one to 2 min after late telophase and remained visible for about 5 min. During this time, small microfilament fragments or monomeric actin originating from the ring depolymerization in the hypha moved to the site where the clamp cell tip fuses with the subapical cell. The microfilaments are involved in the transport of vesicles for building a peg at the side of the subapical cell for fusion with the clamp cell tip (Badalyan et al., 2004; Schubert et al., 2006). An opening is formed and the nucleus enclosed in the clamp cell moves into the subapical cell as is also seen in the living dikaryotic hyphae on plant leaves in the dimorphic phytopathogenic basidiomycete *Ustilago maydis* (Scherer et al., 2006). In Lat A-treated dikaryotic apical cells, the number of clamp cells with an enclosed nucleus was higher than in control hyphae indicating that the nuclear movement from the clamp cell into the subapical cell was inhibited in the absence of actin filaments. The clamp cells with enclosed nuclei represented the last ones formed at the base of the apical cell before the Lat A treatment, in which the nucleus remained trapped due to the start of the Lat A exposure. This shows that actin has an important role in the formation of an opening between the clamp cell tip and the subapical cell, although the actual movement of the nucleus through the opening into the subapical cells follows microtubule tracks (Raudaskoski et al., 1991). The formation of the opening for the movement took

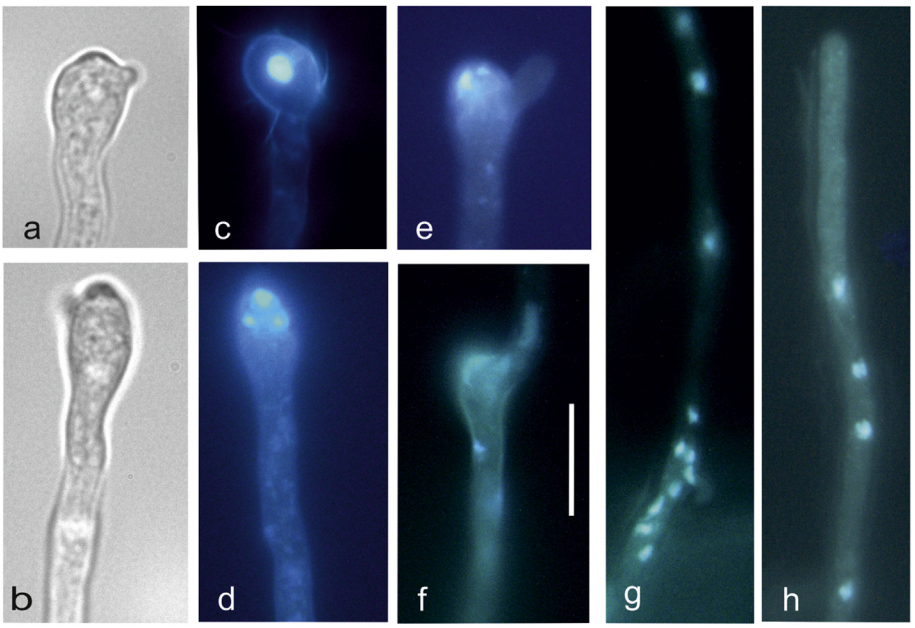

Fig. 9. Recovery of *Schizophyllum commune* dikaryon 1794-114-10 × 684 from 2 h Lat A treatment. The hyphae were fixed and observed by using bright field microscopy (a,b) or the nuclei of the apical cells were stained with Hoechst (c,d,e) or DAPI (f,g,h). (a,b) Swollen tips with small outgrowths and (c,d) nuclei, 2 h recovery. (e–f) Dividing nuclei and nuclear movement (f) into the extensions with polarized tip growth, 4 h recovery. (g-h) Multinucleate polarized hyphae extending from the swollen tips, 8 h recovery. Bar 10 μm.

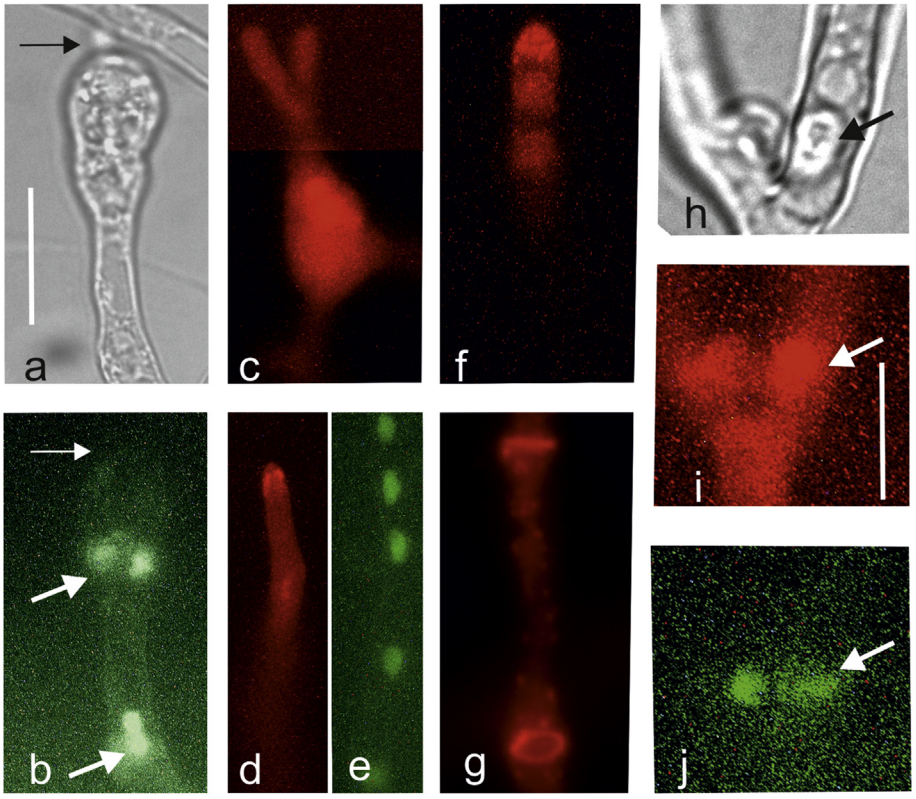

Fig. 10. Recovery from Lat A treatment in *Schizophyllum commune*. Dikaryon 1–11H2B::EGFP × ura 7-3-Lifeact-mCherry was treated with Lat A for 1 h and the monokaryotic (haploid) strain 1792-114-10 for 2 h. The recovery of the living hyphae was recorded from 4 h to 7 h. (a) The swollen hyphal tip with a small out growth (black arrow) and (b) nuclei migrating into the swollen part (white arrows), 7 h recovery. (c) A branched extension with polarized growth from the top and one at the right side with weak Lifeact-mCherry fluorescence at the polarized tips but strong fluorescence in the swollen part, 6 h recovery. (d) A thin hypha with Lifeact-mCherry fluorescence at the tip and (e) a multinucleate hypha, 6 h recovery. (f–g) Indirect immunofluorescence microscopy of the actin cytoskeleton at the hyphal tip (f) and actin rings (g) in a monokaryotic hypha from strain 1792-114-10, 2 h Lat A treatment and 4 h recovery. (h–i) Incomplete clamp cell formation (h) in two branches of a living hypha with LIfeact-mCherry fluorescence (i) and nuclei (j) in the incomplete clamp cells without contractile actin rings, 6 h recovery. Bars 10 μm a–g, 5 μm h–j.

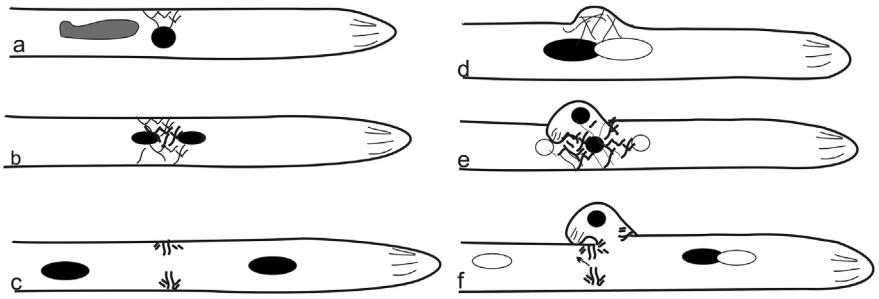

Fig. 11. A schematic drawing of the interaction of nuclei (black and white ellipses) and microfilaments (actin filaments, hairlines with different thickness) in monokaryotic (haploid) (a–c) and dikaryotic (d–f) hyphae during karyokinesis and early cytokinesis preceding septation. (a and d) At the beginning of karyokinesis microfilaments locate the nuclei at the site of division. In the monokaryotic hypha (a) the released part of the nuclear membrane is shown as grey material next to the condensed nucleus. (b and e) At telophase microfilaments polymerize between the sister nuclei. (c and f) At early cytokinesis microfilaments assemble to the contractile actin rings at the plasma membrane, in dikaryotic hyphae microfilaments also occur at the tip of the clamp cell and polymerize to form the peg in the subapical cell (arrow).

13 min from the time the two contractile actin rings were seen, one at the base of the developing clamp cell and the other in the hypha. In dikaryotic hyphae the fusion of the clamp cell with the subapical cell and the nuclear migration into the subapical cell require the presence of G protein-coupled receptors and pheromones encoded by different *B* mating-type genes (Erdmann et al., 2012). The inhibition on the fusion of the clamp cell with the subapical cell by Lat A treatment suggests that the actin cytoskeleton is, at least indirectly, under control of the *B* mating-type genes.

4.3. What is the signal from the nuclear division for the contractile actin ring assembly

In *Schizosacharomyces pombe*, the nucleus and anillin Mid1 protein mark the position of the actin ring at the early stages of mitosis (Paoletti and Chang, 2000; Rincon and Paoletti, 2012). Unfortunately, no Mid proteins are found in the genome of in *S. commune*. In *S. pombe* the septation initiation network (SIN) also regulates the assembly and contraction of the actin ring and the deposition of septum material. The SIN proteins are homologous with proteins found in the Hippo pathway of animal cell and in *Saccharomyces cerevisiae* MEN (mitotic exit network) pathways regulating the cytokinesis (Johnson et al., 2012). The universal conservation of the pathways has led to the identification of homologous proteins in filamentous fungi, *A. nidulans* (Bruno et al. 2001; Kim et al., 2006, 2009), *N. crassa* (Heilig et al., 2013, 2014) and *Sordaria macrospora* (Radchenko et al., 2018), but also in the dimorphic basidiomycete *U. maydis* (Böhmer et al., 2009). The deletion of the SIN pathway proteins in these fungi leads to aseptation, indicating that these proteins are involved in septal formation in filamentous fungi. In the *S. commune* genome, as well, most SIN proteins are found and they have a high level of homology with the *S. pombe* SIN proteins. One of these proteins is the small GTPase Spg1, high levels of which are expressed in the *S. commune* monokaryotic and dikaryotic hyphae (Ohm et al., 2010; Raudaskoski et al., 2011).

In *S. pombe,* Spg1 is bound to the spindle pole body (SPB) and plays a central role in mitosis and cytokinesis. It occurs in active, GTP binding form at both spindle poles bodies during early mitosis, but during spindle development it becomes inactivated at the “old” spindle pole body. At the “new” pole GTP bound Spg1 activates through its effector kinase Cdc7 downstream kinases Sid1 and Sid2. The latter kinase and its cofactor Mob1 move from the SPB to activate proteins in the contractile ring formation through phosphorylation (Johnson et al., 2012). It could be speculated that in *S. commune*, the filamentous actin visualized by Lifeact-mCherry between the late anaphase/early telophase nuclei could be the target for contractile actin ring arrangement and contraction, perhaps through SIN pathway proteins at the SPBs exposed at this stage of division (Runeberg et al., 1986; Raudaskoski et al., 1991). However, in the dimorphic basidiomycete *U. maydis* the deletion of Spg1 resulted in a defect in the nuclear envelope breakdown during early mitosis of the budding cells (Sandrock et al., 2006) and in *A. nidulans* and *N. crassa*, SIN pathway proteins were visualized at SPB but not in a cell cycle-dependent way and as opposed to *S. pombe*, SIN protein activity was not bound to SPB localization (Kim et al., 2009; Heilig et al., 2013, 2014). The SPB in filamentous basidiomycetes has a unique structure (Girbardt, 1971; Raudaskoski, 1972) which has not been analyzed at a molecular level neither the localization of the Spg1 at the SPB has yet been proved.

4.4. Latrunculin treated apical cells

As a consequence of depolarization of actin filaments by Lat A in *S. commune*, polarized hyphal tip growth was replaced by isotropic growth as in *A. nidulans* (Taheri-Talesh et al., 2008). In spite of the change of the tip growth pattern from polarized to isotropic the Lat A-treated apical cells were longer than the apical cells of control hyphae due to the inhibition of the polymerization of the contractile actin ring. Effective blocking of the actin ring with Lat A treatment has also been reported in *U. maydis* and *N. crassa* (Böhmer et al., 2009; Delgado-Alvarez et al., 2010). The accumulation of calcofluor white patches in the swollen tips suggested either synthesis or transport of calcofluor white positive material at the swollen area. This may take place along microtubules, which were shown to exist in Lat A-treated hyphae by indirect immunofluorescence microscopy, although in a reoriented manner. During recovery from Lat A treatment, the calcofluor white patches disappeared and one or several hyphal tips developed from the swollen tip with polarized growth and actin in the tip region. The recovery of the polarized tip growth was preceded by the migration of the nuclei into the swollen hyphal tip which did not occur in the presence of Lat A. This result is different to the one reported in *N. crassa* in which the destabilizing of actin with cytochalazin A led to the movement of nuclei to the hyphal tip (Ramos-García et al., 2009). The nuclear movement into the swollen hyphal apex at release from the Lat A treatment in *S. commune* suggests that there is an interaction between the MT and actin cytoskeleton not only in regulating the hyphal tip growth (Takeshita et al., 2014) but also affecting the nuclear movements.

In Lat A-treated hyphae the nuclear pairing typical to the dikaryotic control hyphae was missing. This indicates that the actin cytoskeleton is needed to keep the nuclei with different mating-

type genes paired. During recovery, the multinucleate branches with a mixture of nuclei with different mating-type genes were observed, the situation was similar to the beginning of mating when extensive reciprocal exchange and migration of nuclei takes place between the compatible strains induced by the presence of different *B* mating-type genes. During mating, the nuclei with different mating type genes gradually become paired and the formation of septum is associated with nuclear division (Raudaskoski, 1973, 1998). The loss of nuclear pairing could explain why the recovery of dikaryotic hyphae after Lat A treatment took much longer time, over 24 h or more, than that of haploid hyphae. It also emphasizes that the actin cytoskeleton plays an important role in association with microtubules in maintaining the pairing of the nuclei with different mating-type genes during dikaryotic growth.

5. Conclusions

In the basidiomycete *S. commune*, the actin cytoskeleton is necessary for polarized tip growth and formation of the septa as it is in other filamentous fungi. In the monokaryotic (haploid) and dikaryotic hyphae of *S. commune* the hyphal septation is closely connected to nuclear division, and the assembly of the contractile actin ring, preceding the septum formation, occurs in a minute or in a less time after telophase movement has separated the sister nuclei. The actin cytoskeleton is also involved in the positioning the nucleus in monokaryotic and the nuclear pair in dikaryotic hyphae in the middle of the apical cell for karyokinesis and cytokinesis (Fig. 11). The signals for the nuclear location or the activation of the actin ring assembly need still to be identified. The actin cytoskeleton keeps the nuclei with different mating-type genes paired in the growing dikaryotic hyphae, the polymerization of the contractile ring regulates the formation of septa, which have a central role in maintaining the mono- and dikaryotic nuclear number of the hyphae. Actin also plays a role in the fusion of the clamp cell with the subapical cell for nuclear migration from the clamp cell into the subapical cell. Nuclear pairing is regulated by *A* and nuclear migration by *B* mating-type genes which indicates that the actin cytoskeleton could be a downstream target for the mating-type genes. Disruption of actin cytoskeleton with Lat A confirmed the involvement of actin filaments in the reported processes.

Acknowledgments

This work was supported by grants from the Finnish Cultural Foundation (the Regional Fund of Southwest Finland) and the Finnish Society of Sciences and Letters. Dr. Jari Korhonen assisted with confocal microscopy and Dr. Mika Keränen with image processing, which I highly appreciate. I would also like to thank PhD student Julia Walter for her help with processing the material into publishable form.

Appendix A. Supplementary data

Supplementary data to this article can be found online at https://doi.org/10.1016/j.funbio.2019.05.009.

References

Badalyan, S.M., Polak, E., Hermann, R., Aebi, M., Kües, U., 2004. Role of peg formation in clamp cell fusion of homobasidiomycete fungi. J. Basic Microbiol. 44, 167–177.

Bruno, K.S., Morrell, J.L., Hamer, J.E., Staiger, C.J., 2001. SEPH, a Cdc7p orthologue from *Aspergillus nidulans*, functions upstream of actin ring formation during cytokinesis. Mol. Microbiol. 42, 3–12.

Brunsch, M., Schubert, D., Gube, M., Ring, C., Hanisch, L., Linde, J., Krause, K., Kothe, E., 2015. Dynein heavy chain, encoded by two genes in Agaricomycetes, is required for nuclear migration in *Schizophyllum commune*. PLoS One 10, e0135616.

Böhmer, C., Ripp, C., Bölker, M., 2009. The germinal centre kinase Don3 triggers the dynamic rearrangement of higher-order septin structures during cytokinesis in *Ustilago maydis*. Mol. Microbiol. 74, 1484–1496.

Delgado-Alvarez, D.L., Callejas-Negrete, O.A., Gómez, N.M., Freitag, M., Roberson, R.W., Smith, L.G., Mouriño-Pérez, R.R., 2010. Visualization of F-actin localization and dynamics with live cell markers in *Neurospora crassa*. Fungal Genet. Biol. 47, 573–586.

Delgado-Álvarez, D.L., Bartnicki-García, S., Seiler, S., Mouriño-Pérez, R.R., 2014. Septum development in *Neurospora crassa*: the septal actomyosin tangle. PLoS One 9, e96744.

Erdmann, S., Freihorst, D., Raudaskoski, M., Schmidt-Heck, W., Jung, E.-M., Senftleben, D., Kothe, E., 2012. Transcriptome and functional analysis of mating in the basidiomycete *Schizophyllum commune*. Eukaryot. Cell 11, 5571–5589.

Girbardt, M., 1968. Ultrastructure and dynamics of the moving nucleus. In: Miller, P.L. (Ed.), Aspects of Cell Motility. Symp. Soc. Exp. Biol., vol. 22. University Press, Cambridge, pp. 249–259.

Girbardt, M., 1971. Ultrastructure of the fungal nucleus II. The kinetochore equivalent (KCE). J. Cell Sci. 2, 453–473.

Girbardt, M., 1979. A microfilamentous septal belt (FSB) during induction of cytokinesis in *Trametes versicolor*. Exp. Mycol. 3, 215–228.

Heilig, Y., Schmitt, K., Seiler, S., 2013. Phosphoregulation of the *Neurospora crassa* septation initiation network. PLoS One 8, e79464.

Heilig, Y., Dettmann, A., Mouriño-Pérez, R.R., Schmitt, K., Valerius, O., Seiler, S., 2014. Proper actin ring formation and septum constriction requires coordinated regulation of SIN and MOR pathways through the germinal centre kinase MST-1. PLoS Genet. 24, e1004306.

Johnson, A.E., McCollum, D., Gould, K.L., 2012. Polar opposites: fine-tuning cytokinesis through SIN asymmetry. Cytoskeleton (Hoboken) 69, 686–699.

Jung, E.M., Kothe, E., Raudaskoski, M., 2018. The making of a mushroom: mitosis, nuclear migration and the actin network. Fungal Genet. Biol. 111, 85–91.

Kamada, T., Tanabe, S., 1995. The role of cytoskeleton in the movement and positioning of nuclei in *Coprinus cinereus*. Can. J. Bot. 73 (Suppl. 1), S364–S368.

Kim, J.M., Lu, L., Shao, B., Chin, J., Liu, B., 2006. Isolation of mutations that bypass the requirement of the septation initiation network for septum formation and conidiation in *Aspergillus nidulans*. Genetics 173, 685–696.

Kim, J.M., Zeng, C.J., Nayak, T., Shao, R., Huang, A.C., Oakley, B.R., Liu, B., 2009. Timely septation requires SNAD-dependent spindle pole body localization of the septation initiation network components in the filamentous fungus *Aspergillus nidulans*. Mol. Biol. Cell. 20, 2874–2884.

Ohm, R.A., de Jong, J.F., Lugones, L.G., Aerts, A., Kothe, E., Stajich, J.E., de Vries, R.P., Record, E., Levasseur, A., Baker, S.E., Bartholomew, K.A., Coutinho, P.M., Erdmann, S., Fowler, T.J., Gathman, A.C., Lombard, V., Henrissat, B., Knabe, N., Kües, U., Lilly, W.W., Lindquist, E., Lucas, S., Magnuson, J.K., Piumi, F., Raudaskoski, M., Salamov, A., Schmutz, J., Schwarze, F.W., vanKuyk, P.A., Horton, J.S., Grigoriev, I.V., Wösten, H.A.B., 2010. Genome sequence of the model mushroom *Schizophyllum commune*. Nat. Biotechnol. 28, 957–963.

Paoletti, A., Chang, F., 2000. Analysis of mid 1p, a protein required for placement of the cell division site, reveals a link between the nucleus and the cell surface in fission yeast. Mol. Biol. Cell 11, 2757–2773.

Radchenko, D., Teichert, I., Pöggeler, S., Kück, U.A., 2018. Hippo pathway-related GCK controls both sexual and vegetative developmental processes in the fungus *Sordaria macrospora*. Genetics 210, 137–153.

Ramos-García, S.L., Roberson, R.W., Freitag, M., Bartnicki-García, S., Mouriño-Pérez, R.R., 2009. Cytoplasmic bulk flow propels nuclei in mature hyphae of *Neurospora crassa*. Eukaryot. Cell 8, 1880–1890.

Raper, J., 1966. Sexuality of Higher Fungi. Ronald Press, New York.

Raper, J.R., Raudaskoski, M., 1968. Secondary mutations at the *Bβ* incompatibility locus of *Schizophyllum*. Heredity 23, 109–117.

Raudaskoski, M., 1972. Occurrence of microtubules in the hyphae of *Schizophyllum commune* during intercellular nuclear migration. Arch. Mikrobiol. 86, 91–100.

Raudaskoski, M., 1973. Light and electron microscope study of unilateral mating between a secondary mutant and a wild-type strain of *Schizophyllum commune*. Protoplasma 76, 35–48.

Raudaskoski, M., 1998. The relationship between *B*-mating-type genes and nuclear migration in *Schizophyllum commune*. Fungal Genet. Biol. 24, 207–227.

Raudaskoski, M., 2015. Mating-type genes and hyphal fusions in filamentous basidiomycetes. Fungal Biol. Rev. 29, 179–193.

Raudaskoski, M., Viitanen, H., 1982. Effect of aeration and light on fruit body induction in *Schizophyllum commune*. Trans. Br. Mycol. Soc. 78, 89–96.

Raudaskoski, M., Yli-Mattila, T., 1985. Capacity for photoinduced fruiting in a dikaryon of *Schizophyllum commune*. Trans. Br. Mycol. Soc. 85, 145–151.

Raudaskoski, M., Rupes, I., Timonen, S., 1991. Immunofluorescence microscopy of the cytoskeleton in filamentous fungi after quick-freezing and low-temperature fixation. Exp. Mycol. 15, 167–173.

Raudaskoski, M., Mao, W.Z., Yli-Mattila, T., 1994. Microtubule cytoskeleton in hyphal growth. Response to nocodazole in a sensitive and a tolerant strain in the homobasidiomycete *Schizophyllum commune*. Eur. J. Cell Biol. 64, 131–141.

Raudaskoski, M., Salo, V., Uuskallio, M., 2009. Kinesin genes and nuclear migration in the basidiomycete *Schizophyllum commune*. 25th fungal genetics conference at asimolar. In: Comparative Function of Genomics. Poster, 8, p. 122.

Raudaskoski, M., Kothe, E., 2010. Basidiomycete mating type genes and pheromone signaling. Eukaryot. Cell 9, 847–859.

Raudaskoski, M., Kothe, E., Fowler, T.J., Jung, E.M., Horton, J.S., 2011. Ras and Rho small G proteins: insights from the *Schizophyllum commune* genome sequence and comparisons to other fungi. Biotechnol. Genet. Eng. Rev. 28, 61–100.

Rincon, S.A., Paoletti, A., 2012. Mid1/Anillin and the spatial regulation of cytokinesis in fission yeast. Cytoskeleton 69, 764–777.

Riquelme, M., Aguirre, J., Bartnicki-García, S., Braus, G.H., Feldbrügge, M., Fleig, U., Hansberg, W., Herrera-Estrella, A., Kämper, J., Kück, U., Mouriño-Pérez, R.R., Takeshita, N., Fischer, R., 2018. Fungal morphogenesis, from the polarized growth of hyphae to complex reproduction and infection structures. Microbiol. Mol. Biol. Rev. 82 e00068–17.

Runeberg, P., Raudaskoski, M., Virtanen, I., 1986. Cytoskeletal elements in the hyphae of the homobasidiomycete *Schizophyllum commune* visualized with indirect immunofluorescence and NBD phallacidin. Eur. J. Cell Biol. 41, 25–32.

Sandrock, B., Böhmer, C., Bölker, M., 2006. Dual function of the germinal centre kinase Don3 during mitosis and cytokinesis in *Ustilago maydis*. Mol. Microbiol. 62, 655–666.

Shen, K.F., Osmani, A.H., Govindaraghavan, M., Osmani, S.A., 2014. Mitotic regulation of fungal cell-to-cell connectivity through septal pores involves the NIMA kinase. Mol. Biol. Cell 25, 763–775.

Scherer, M., Heimel, K., Starke, V., Kämper, J., 2006. The Clp1 protein is required for clamp formation and pathogenic development of *Ustilago maydis*. Plant Cell 18, 2388–2401.

Schubert, D., Raudaskoski, M., Knabe, N., Kothe, E., 2006. Ras GTPase-activating protein Gap1 of the homobasidiomycete *Schizophyllum commune* regulates hyphal growth orientation and sexual development. Eukar. Cell 5, 683–695.

Schuren, F.H.J., Wessels, J.G.H., 1994. Highly efficient transformation of the homobasidiomycete *Schizophyllum commune* to phleomycin resistance. Curr. Genet. 26, 179–183.

Snider, P.J., 1968. Nuclear movements in Schizophyllum. In: Miller, P.L. (Ed.), Aspects of Cell Motility. Symp. Soc. Exp. Biol, 22. University Press, Cambridge, pp. 261–283.

Steinberg, G., Peñalva, M.A., Riquelme, M., Wösten, H.A., Harris, S.D., 2017. Cell biology of hyphal growth. Microbiol. Spectr. 5 https://doi.org/10.1128/microbiolspec.FUNK-0034-2016.

Taheri-Talesh, N., Horio, T., Araujo-Bazán, L., Dou, X., Espeso, E.A., Peñalva, M.A., Osmani, S.A., Oakley, B.R., 2008. The tip growth apparatus of *Aspergillus nidulans*. Mol. Biol. Cell 19, 1439–1449.

Taheri-Talesh, N., Xiong, Y., Oakley, B.R., 2012. The functions of myosin II and myosin V homologs in tip growth and septation in *Aspergillus nidulans*. PLoS One 7, e31218.

Takeshita, N., Manck, R., Grün, N., de Vega, S.H., Fischer, R., 2014. Interdependence of the actin and the microtubule cytoskeleton during fungal growth. Curr. Opin. Microbiol. 20, 34–41.

Tanabe, S., Kamada, T., 1996. Dynamics of the actin cytoskeleton, hyphal tip growth and the movement of the two nuclei in the dikaryon of *Coprinus cinereus*. Mycoscience 37, 339–344.

Weber, M., Salo, V., Uuskallio, M., Raudaskoski, M., 2005. Ectopic expression of a constitutively active Cdc42 small GTPase alters the morphology of haploid and dikaryotic hyphae in the filamentous homobasidiomycete *Schizophyllum commune*. Fungal Genet. Biol. 42, 624–637.